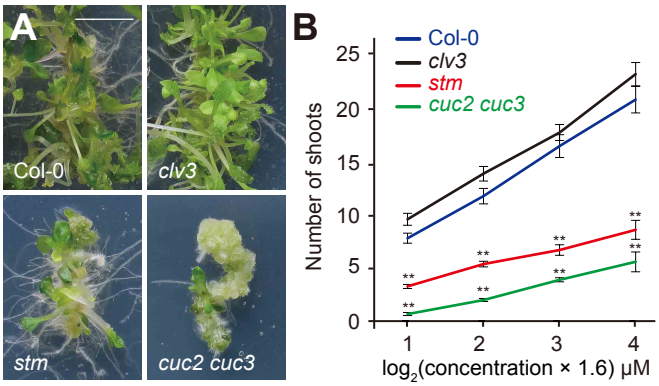

Supplemental Figure 1. Shoot Regeneration in *clv3*, *stm* and *cuc2 cuc3*. (Supports Figure 1).

The regenerative capacity in **(A)** was calculated as the number of shoots/total number of explants. Data are expressed as mean ± s.d.. *n*=24; p-value: Student's *t* test; **p<0.01. Bar = 0.5 cm.

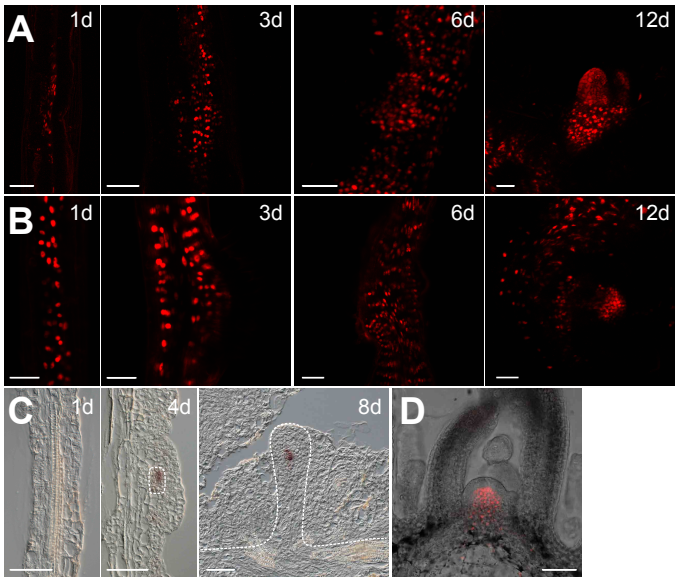

Supplemental Figure 2. Comparison of the Expression Patterns of *WUS* Reporters. (Supports Figure 1).

(A) and **(D)** The expression pattern of *ProWUS:dsRED-N7* (Gordon et al., 2007) reporter during shoot regeneration **(A)** and in the SAM **(D)**. The hypocotyls of *ProWUS:dsRED-N7* were used as explants. During shoot regeneration **(A)**, WUS^{+} cells (red) were visible after 1 day transfer to SIM and did not mark shoot progenitor cells. The difference between the mRNA accumulation pattern revealed by our *in situ* hybridization (Figures 1D to 1I) and protein localization revealed by live imaging analyses of Gordon's *ProWUS:dsRED-N7* reporter is not caused by the movement of DsRED because DsRED was fused to the N7 nuclear localization sequence. We speculate that the difference between our and Gordon's *WUS* reporter was due to the *35S* promoter in the binary construct pPZP222 used by Gordon et al (Gordon et al., 2007). However, this reporter does mimic endogenous *WUS* expression pattern in the SAM **(D)**. Bar = 50 μm.

(B) The expression pattern of *ProWUS:dsRED-N7* (Gordon et al., 2007) reporter on SIM. The roots were used as explants. Bar = 50 μm.

(C) RNA *in situ* hybridization analyses. The roots of *ProWUS:dsRED-N7* were used as explants. Note when comparing **(B)** and **(C)**, it appears that *ProWUS:dsRED-N7* reporter does not mimic the *WUS* mRNA expression pattern. Bar = 50 μm.

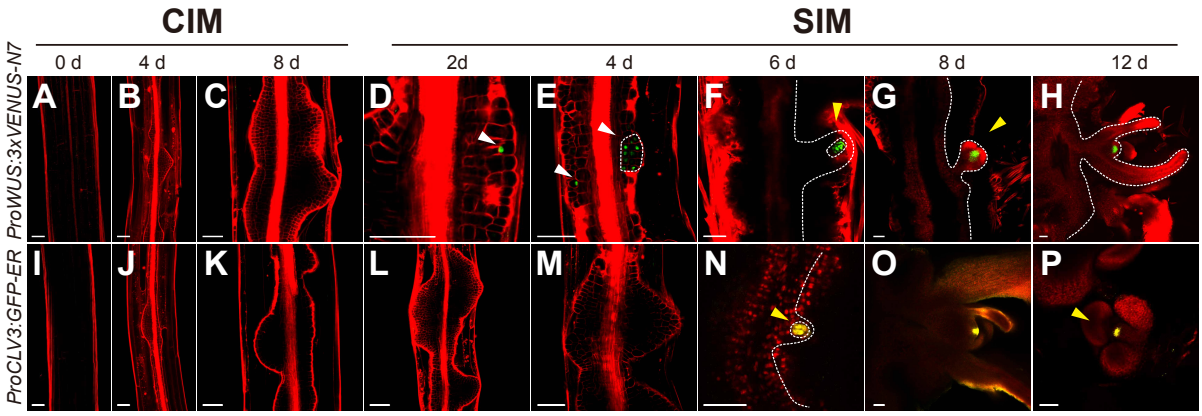

Supplemental Figure 3. Dynamic Expression Patterns of *WUS and CLV3* during Shoot Regeneration. (Supports Figure 1).

Hypocotyls from *ProWUS:3xVENUS-N7* **(A)** to **(H)** and *ProCLV3:GFP-ER* **(I)** to **(P)** were used for shoot regeneration. White and yellow arrows indicate WUS^{+} cell and the developing SAM respectively. Cell outlines were stained by propidium iodide (PI, red). Bar = 50 μm.

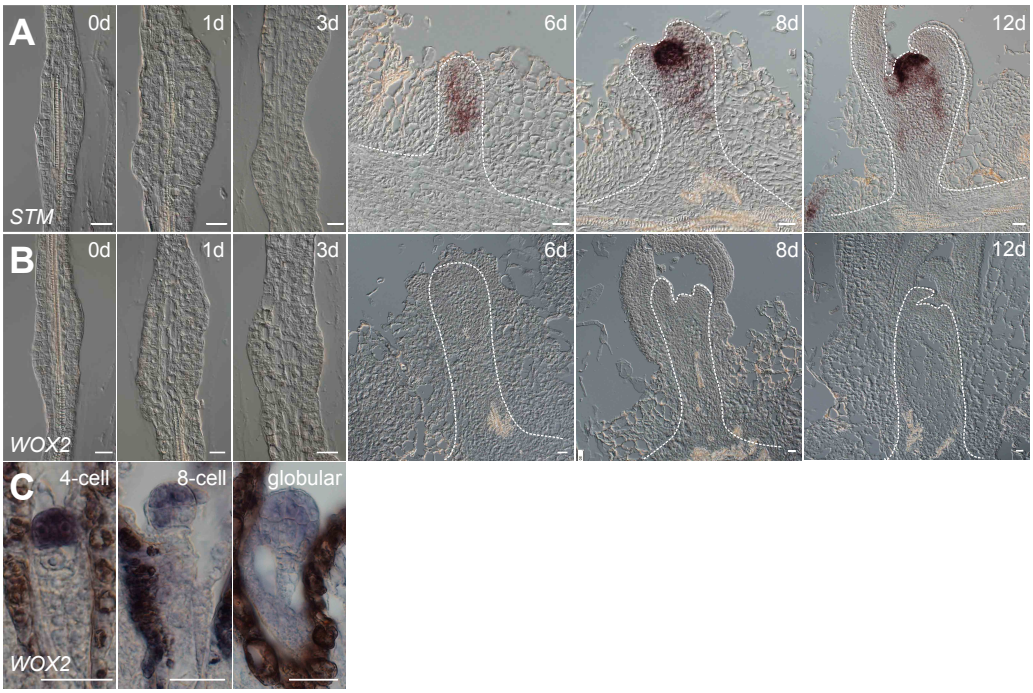

Supplemental Figure 4. Expression Patterns of *STM* and *WOX2*. (Supports Figure 1).

(A) Expression of *STM* is detectable beginning at stage III during shoot regeneration. Bar = 20 μm. **(B)** and **(C)** The transcripts of *WOX2* (blue) could be detected in the proembryo during embryogenesis **(C)** but not in calli during shoot *de novo* regeneration **(B)**. Bar = 20 μm.

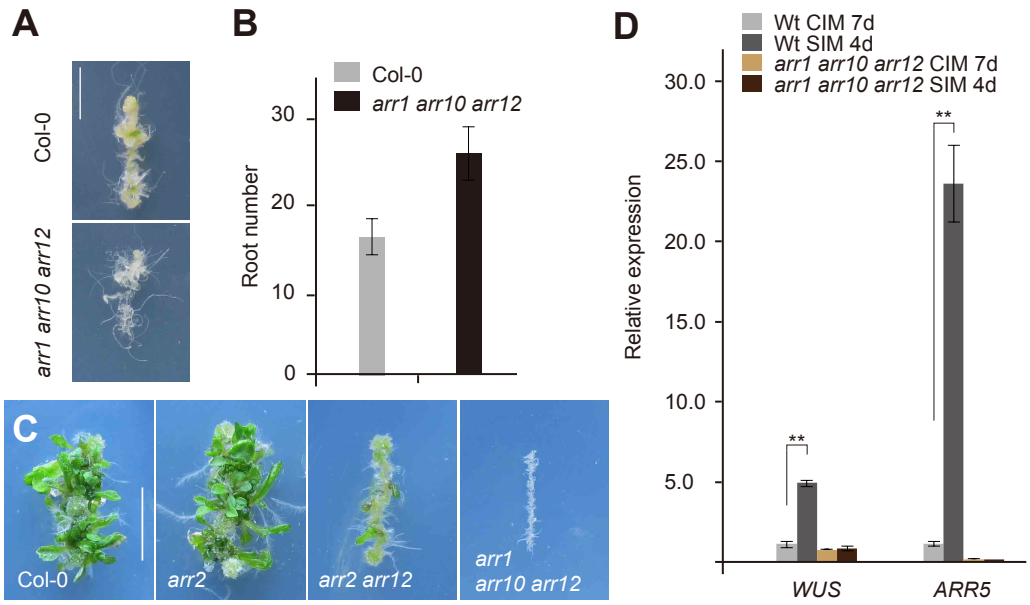

Supplemental Figure 5. Regeneration Assay in the *arr* Mutant. (Supports Figure 2).

(A) and **(B)** The hypocotyls of wild type and *arr1 arr10 arr12* mutant were used for the root regeneration assay. Note that the loss of function of *B-ARRs* did not affect root regenerative capacity. The regenerative capacity in **(B)** was calculated as the number of rooted explants/total number of explants. Data are expressed as mean ± s.d.. *n*=32; Bar = 0.5 cm.

(C) Shoot regeneration of wild type (Col-0), *arr2*, *arr2 arr12* and *arr1 arr10 arr12*. While *arr2* and *arr12* single mutant regenerated shoots normally (Mason et al., 2005), *arr2 arr12* double mutant showed reduced shoot regenerative capacity. Bar = 0.5 cm.

(D) The expression level of *WUS* and *ARR5* in the wild-type and *arr1 arr10 arr12* explants. The expression of *WUS* and *ARR5* in wild type was normalized to that of *TUB*. Data are means ± s.d.. *n*=3. Student's *t* test; **p<0.01.

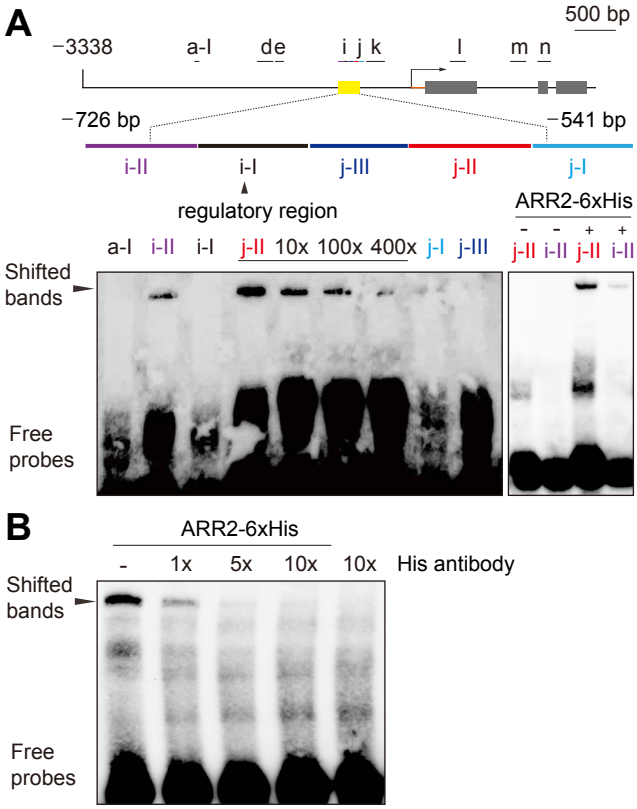

Supplemental Figure 6. EMSA Assays. (Supports Figure 2).

(A) EMSA assays. Competitive EMSA showing binding of ARR2 to two DNA fragments [-550 to -620 bp (j-II) and -700 to -760 bp (i-II)] of the *WUS* promoter (left panel). Relative amounts (labeled oligonucleotide was set to 1.0) of the un-labeled competitive oligonucleotide used in the reactions are indicated on the top. The positions of probes (a-I, i-I, i-II, j-I, j-II, j-III) are labeled with different colors. Shifted bands are indicated. The D5 region (-726 to -541 bp) and a 57-bp regulatory region (-712 to -655 bp, i-I) identified by Bäurle and Laux are shown (Baurle and Laux, 2005). As a control, we performed the EMSA assays without (-) or with (+) ARR2 protein (right panel). Note that there is no shifted band for probe j-II and i-II in the absence of ARR2 protein.

(B) Supershift assays of j-II segment. The purified ARR2 proteins were mixed with different amounts of His antibody. The binding of His antibody with ARR2-6xHis proteins caused the decreased amounts of j-II shifted band.

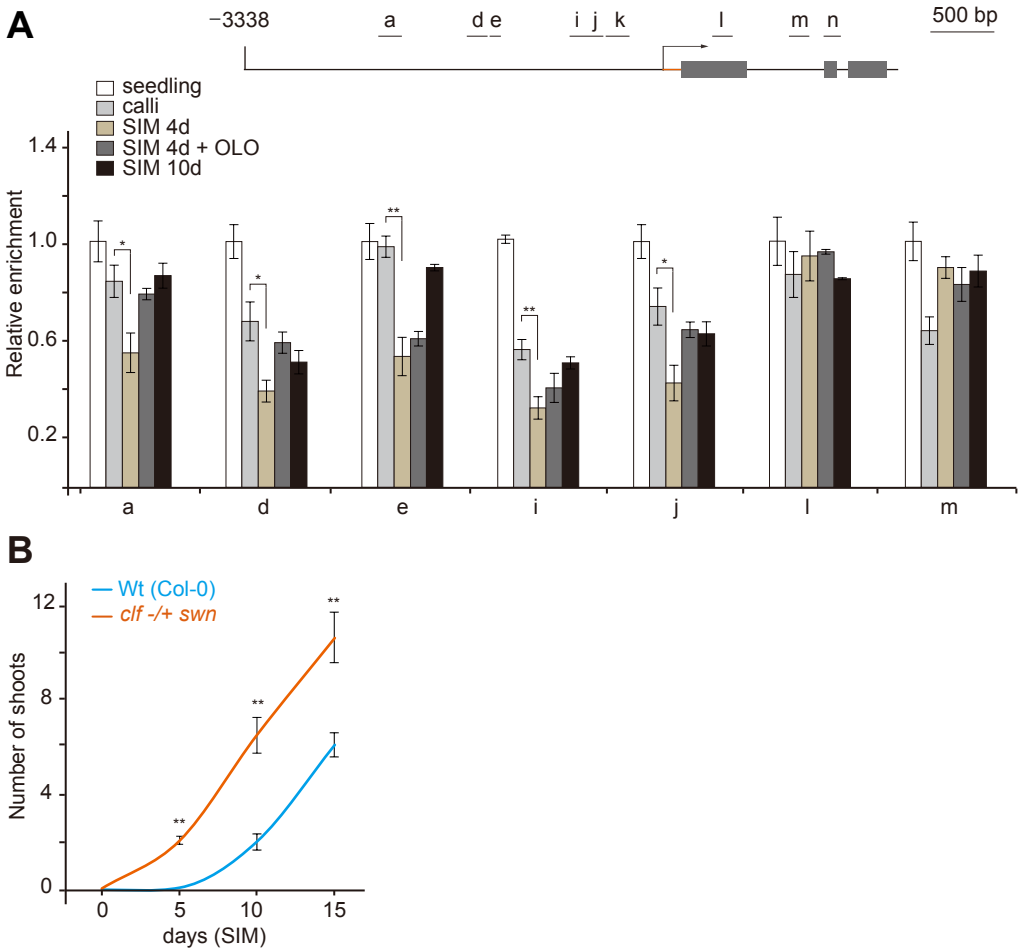

Supplemental Figure 7. The Progressive Decrease in H3K27me3 Marks at the *WUS* Locus is Delayed by OLO Treatment. (Supports Figure 3).

(A) ChIP analyses. Wild-type seedlings and explants cultured on SIM with or without OLO were used. Eight fragments (a to n) were analyzed. Error bars represent s.e.m. (*n*=3 biological replicates); p-value: Student's *t* test; *p<0.05, **p<0.01.

(B) Shoot regeneration of the wild-type (Col-0) and *swn clf* +/- explants. Student's *t* test; **p<0.01, *n*=18.

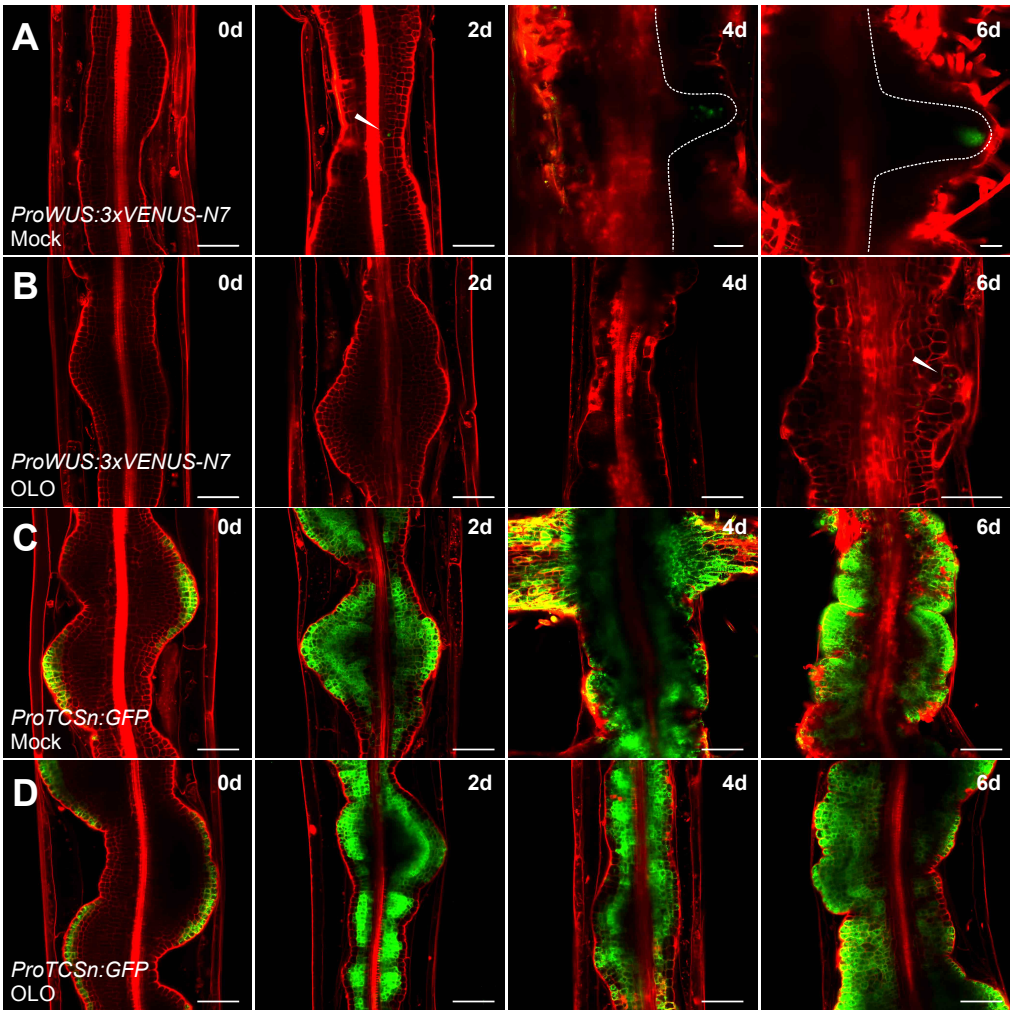

Supplemental Figure 8. The Induction of *WUS* by Cytokinin is Delayed by OLO Treatment. (Supports Figure 3).

(A) to **(D)** The *ProWUS:3xVENUS-N7* and *ProTCSn:GFP* explants were regenerated on SIM with **(B)** and **(D)** or without OLO **(A)** and **(C)**. White arrows indicate WUS^{+} cells. Cell outlines were stained by PI (red). Bar = 50 μm.

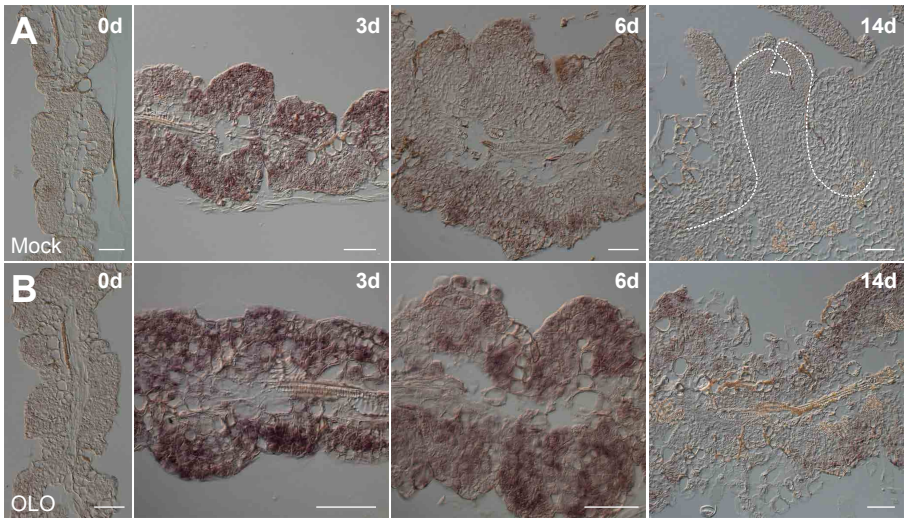

Supplemental Figure 9. The Induction of *ARR5* by Cytokinin is not Delayed by OLO Treatment. (Supports Figure 3).

(A) and **(B)** The expression of *ARR5*. The wild-type explants were regenerated on SIM with **(B)** or without OLO **(A)**. The expression of *ARR5* was analyzed at day 0, 3, 6 and 14. Bar = 50 μm.

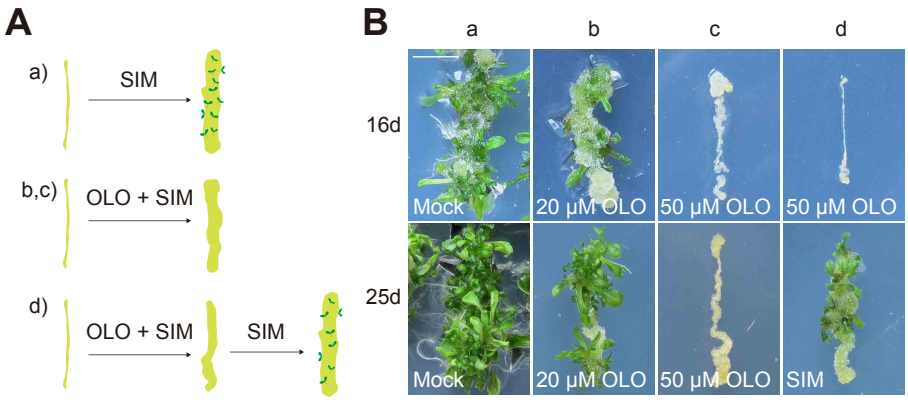

Supplemental Figure 10. The Induction of Shoot Regeneration by Cytokinin is Delayed by OLO Treatment. (Supports Figure 3).

(A) Set-up for the experiment to test the role of cell cycle in shoot regeneration. Four experiments (a-d) were designed.

(B) Shoot regeneration assays according to the experimental designs **(A)**. Bar = 0.5 cm.

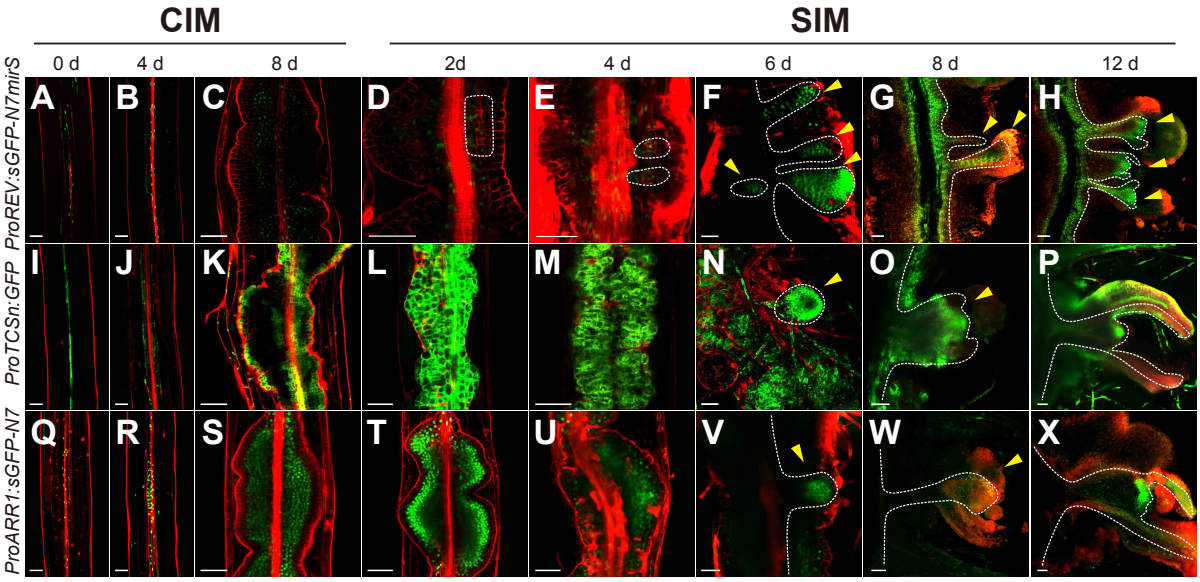

Supplemental Figure 11. Dynamic Expression Patterns of *REV*, *TCS and ARR1* during Shoot Regeneration. (Supports Figures 2, 4 and 7).

The hypocotyls from *ProREV:sGFP-N7mirS* **(A)** to **(H)**, *ProTCSn:GFP* **(I)** to **(P)** and *ProARR1:sGFP-N7* **(Q)** to **(X)** were used for shoot regeneration. Yellow arrows indicate the developing SAM. Cell outlines were stained by propidium iodide (PI, red). Bar = 50 μm.

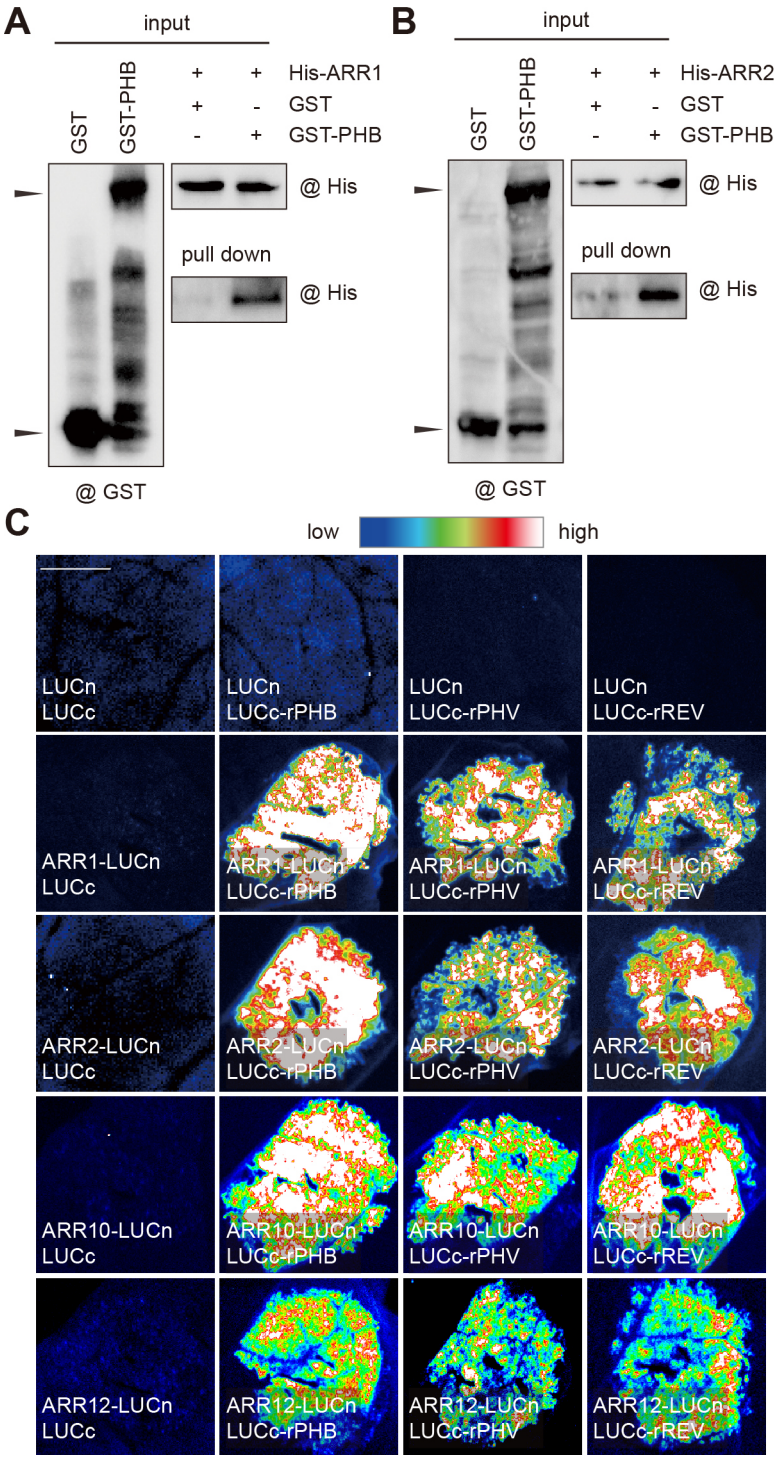

Supplemental Figure 12. ARR1, ARR2, ARR10 and ARR12 Bind to HD-ZIP III Proteins. (Supports Figure 4).

(A) and **(B)** *In vitro* pull-down assay. 6xHis-ARR1, 6xHis-ARR2 and GST-PHB were expressed in *E. coli*. Purified proteins were mixed and immunoprecipitated with glutathione sepharose 4B resins and blotted against anti-His or anti-GST antibody.

(C) BiLC assay in *N. benthamiana* leaves. ARR1, ARR2, ARR10 and ARR12 were fused to the amino-terminal domain of LUC (LUCn) and PHB/PHV/REV fused to the carboxyl-terminal domain of LUC (LUCc). Bar = 1.0 cm.

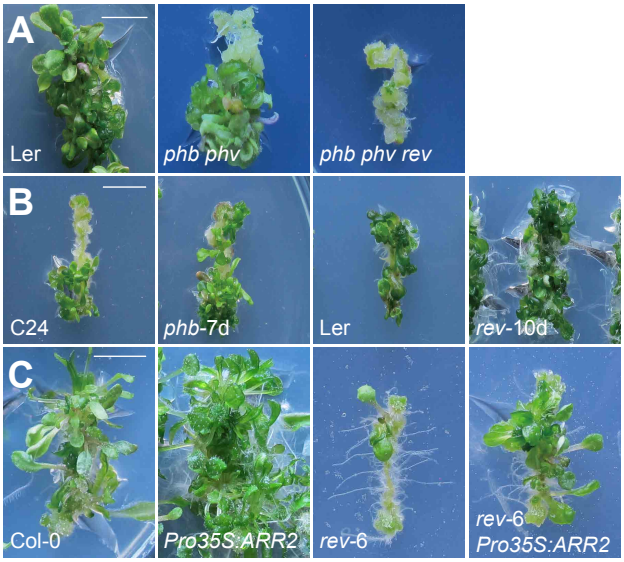

Supplemental Figure 13. Shoot Regeneration Assay of *HD-ZIP III* Mutants. (Supports Figure 4).
(A) and **(B)** Shoot regeneration assay of *HD-ZIP III* mutants. Bar = 0.5 cm.
(C) Shoot regeneration assay of Col-0, *Pro35S:ARR2*, *rev*-6 and *Pro35S:ARR2 rev*-6. Bar = 0.5 cm.

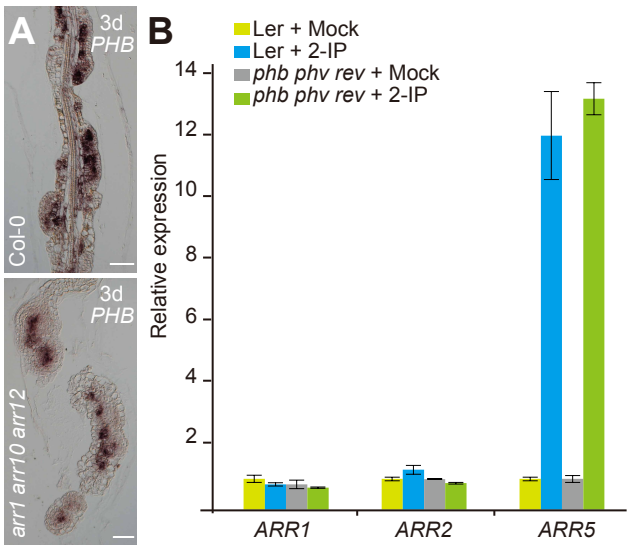

Supplemental Figure 14. Expression of *HD-ZIP III* Transcription Factors and B-type *ARRs*.(Supports Figure 4).

(A) Expression of *PHB* in the wild-type and *arr1 arr10 arr12* explants. The explants were cultured on SIM for 3 days. Bar = 50 μm.

(B) Expression of A-type and B-type *ARRs* in wild type and *phb phv rev* explants. Expression was examined by qRT-PCR and normalized to that of *TUB*. Data are means ± s.d.. *n*=3.

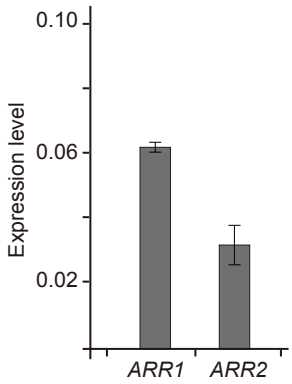

Supplemental Figure 15. Expression of *ARR1* and *ARR2* in Wild-Type Explants. (Supports Figure 6).

Expression was examined by qRT-PCR and normalized to that of *TUB*. Data are means ± s.d.. *n*=3.

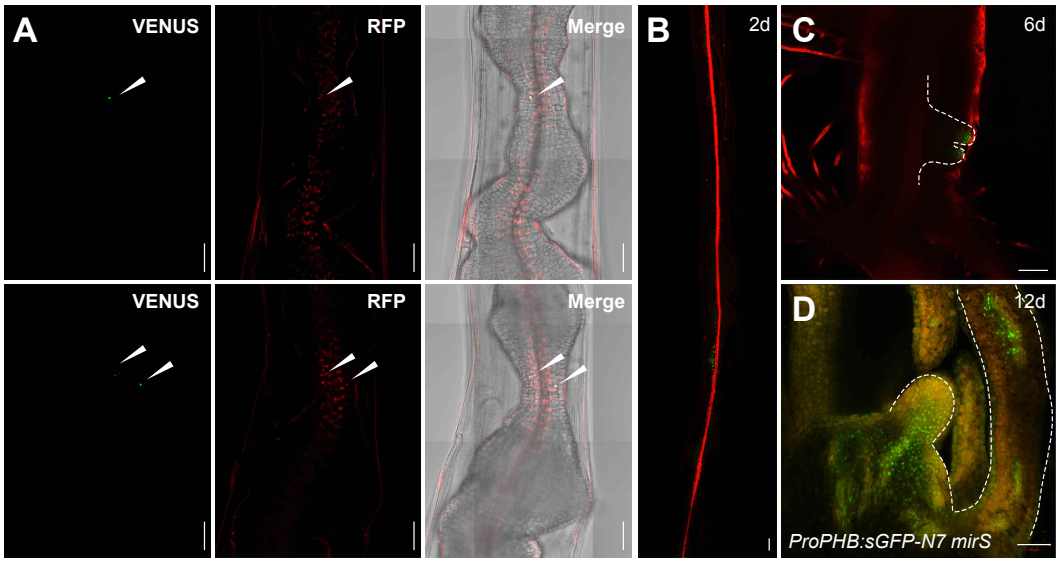

Supplemental Figure 16. Spatial Activation of *WUS* by REV and PHB. (Supports Figure 7).
(A) Expression of *ProREV:DsRED-N7 mirS ProWUS:3xVENUS-N7*. The explant was cultured on SIM for 2 days. The WUS^{+} cell (green) is indicated by white arrows. Bar = 50 μm.
(B) to **(D)** Expression of *ProPHB:sGFP-N7 mirS* (green). The explants were culture on SIM for 2, 6 and 12 days. The expression domain of *PHB* is marked with dashed lines. Bar = 50 μm.

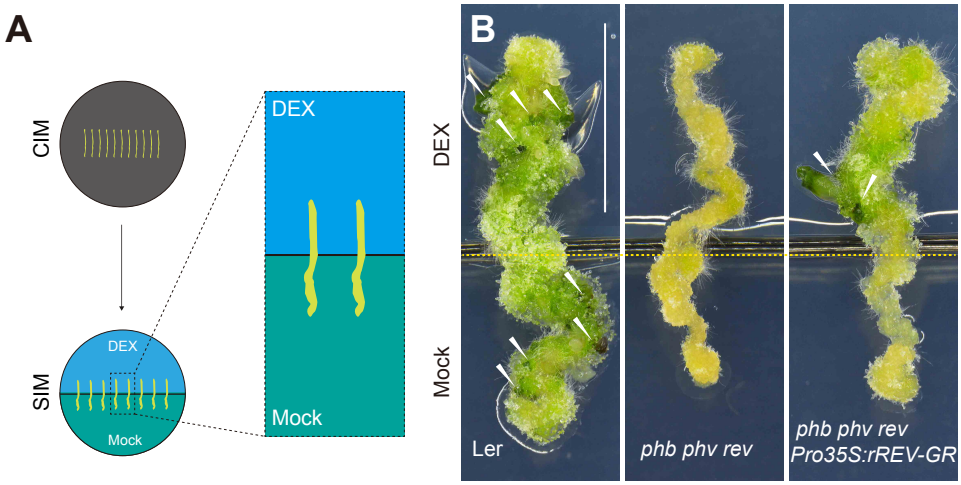

Supplemental Figure 17. Local Induction of *HD-ZIP III* Promotes Shoot Regeneration on SIM. (Supports Figures 4 and 7).

(A) and **(B)** Shoot regeneration assay of wild type (Ler), *phb phv rev* and *phb phv rev Pro35S:rREV-GR*. **(A)** Schematic diagram shows the experimental procedure for local induction of *HD-ZIP III*. A biplate (Thermo fisher, PB5220E) which allows two separate media formulations was used. **(B)** Explants of different genotypes were cultured on SIM with or without 10 μM DEX for 10 days. White arrows indicate regenerated shoots. Bar = 0.5 cm.

Supplemental Figure 18. Genetic Interaction between *ARR2* and *REV* during Shoot Development. (Supports Figures 4 and 7).

(A) Phenotypes of wild type and mutants. Bar = 1 cm. The proportion of transgenic plants showing phenotype is shown.

(B) to **(D)** Expression of *WUS* in wild type and mutants. The *WUS* transcripts were detected by *in situ* hybridization assay. Bar = 50 μm.

Supplemental Table 1. Yeast Two-Hybrid Assay using ARR2 as Bait.

Gene	Interaction?	Biological Function
PHB (At2g34710)	Yes	HD-ZIP III transcription factor, defines adaxial leaf fates (Prigge et al., 2005)
REV (At5g60690)	Yes	HD-ZIP III transcription factor, defines adaxial leaf fates (Prigge et al., 2005)
PHV (At1g30490)	Yes	HD-ZIP III transcription factor, defines adaxial leaf fates (Prigge et al., 2005)
CUC2 (At5g53950)	No	Transcription factor of the *NAC* gene family, required for the embryonic SAM (Daimon et al., 2003)
CUC3 (At1g76420)	No	Transcription factor of the *NAC* gene family, required for embryonic apical meristem formation (Daimon et al., 2003; Vroemen et al., 2003; Hibara et al., 2006)
TCP4 (At3g15030)	No	Target gene of miR319, regulate leaf differentiation (Efroni et al., 2013)
ESR1 (At1g12980)	No	ERF/AP2 transcription factor, regulates shoot regeneration and meristem activity (Banno et al., 2001)
MP (At1g19850)	No	Auxin response factor, play roles in the development of shoot primordia (Zhao et al., 2010)
BRC1 (At3g18550)	No	TCP transcription factor, functions in axillary bud development (Aguilar-Martinez et al., 2007)
TFL2 (At5g17690)	No	TFL2 recognizes specifically H3K27me3 *in vivo* (Turck et al., 2007)
LCR (At1g27340)	No	F-box protein, involved in the regulation of leaf morphology and meristem activity (Knauer et al., 2013)

SUPPLEMENTAL REFERENCES

Aguilar-Martinez, J.A., Poza-Carrion, C., and Cubas, P. (2007). Arabidopsis BRANCHED1 acts as an integrator of branching signals within axillary buds. Plant Cell **19,** 458-472.

Banno, H., Ikeda, Y., Niu, Q.W., and Chua, N.H. (2001). Overexpression of Arabidopsis ESR1 induces initiation of shoot regeneration. Plant Cell **13,** 2609-2618.

Baurle, I., and Laux, T. (2005). Regulation of *WUSCHEL* transcription in the stem cell niche of the Arabidopsis shoot meristem. Plant Cell **17,** 2271-2280.

Daimon, Y., Takabe, K., and Tasaka, M. (2003). The *CUP-SHAPED COTYLEDON* genes promote adventitious shoot formation on calli. Plant Cell Physiol **44,** 113-121.

Efroni, I., Han, S.K., Kim, H.J., Wu, M.F., Steiner, E., Birnbaum, K.D., Hong, J.C., Eshed, Y., and Wagner, D. (2013). Regulation of leaf maturation by chromatin-mediated modulation of cytokinin responses. Dev Cell **24,** 438-445.

Gordon, S.P., Heisler, M.G., Reddy, G.V., Ohno, C., Das, P., and Meyerowitz, E.M. (2007). Pattern formation during *de novo* assembly of the Arabidopsis shoot meristem. Development **134,** 3539-3548.

Hibara, K., Karim, M.R., Takada, S., Taoka, K., Furutani, M., Aida, M., and Tasaka, M. (2006). Arabidopsis *CUP-SHAPED COTYLEDON3* regulates postembryonic shoot meristem and organ boundary formation. Plant Cell **18,** 2946-2957.

Knauer, S., Holt, A.L., Rubio-Somoza, I., Tucker, E.J., Hinze, A., Pisch, M., Javelle, M., Timmermans, M.C., Tucker, M.R., and Laux, T. (2013). A protodermal miR394 signal defines a region of stem cell competence in the Arabidopsis shoot meristem. Dev Cell **24,** 125-132.

Mason, M.G., Mathews, D.E., Argyros, D.A., Maxwell, B.B., Kieber, J.J., Alonso, J.M., Ecker, J.R., and Schaller, G.E. (2005). Multiple type-B response regulators mediate cytokinin signal transduction in Arabidopsis. Plant Cell **17,** 3007-3018.

Prigge, M.J., Otsuga, D., Alonso, J.M., Ecker, J.R., Drews, G.N., and Clark, S.E. (2005). Class III homeodomain-leucine zipper gene family members have overlapping, antagonistic, and distinct roles in Arabidopsis development. Plant Cell **17,** 61-76.

Turck, F., Roudier, F., Farrona, S., Martin-Magniette, M.L., Guillaume, E., Buisine, N., Gagnot, S., Martienssen, R.A., Coupland, G., and Colot, V. (2007). Arabidopsis TFL2/LHP1 specifically associates with genes marked by trimethylation of histone H3 lysine 27. PLoS Genet **3,** e86.

Vroemen, C.W., Mordhorst, A.P., Albrecht, C., Kwaaitaal, M.A., and de Vries, S.C. (2003). The *CUP-SHAPED COTYLEDON3* gene is required for boundary and shoot meristem formation in Arabidopsis. Plant Cell **15,** 1563-1577.

Zhao, Z., Andersen, S.U., Ljung, K., Dolezal, K., Miotk, A., Schultheiss, S.J., and Lohmann, J.U. (2010). Hormonal control of the shoot stem-cell niche. Nature **465,** 1089-1092.